

PPPL-2601

46  
4-13-89

ST (2)

PPPL-2601

UC-427

Doc # C778-1


Sawtooth Oscillation in Tokamaks

By

W. Park and D.A. Monticello

MASTER

MARCH 1989

PLASMA  
PHYSICS  
LABORATORY 

PRINCETON UNIVERSITY  
PRINCETON, NEW JERSEY

PREPARED FOR THE U.S. DEPARTMENT OF ENERGY,  
UNDER CONTRACT DE-AC02-76-CEO-3073.

NOTICE

This report was prepared as an account of work sponsored by the United States Government. Neither the United States nor the United States Department of Energy, nor any of their employees, nor any of their contractors, subcontractors, or their employees, makes any warranty, express or implied, or assumes any legal liability or responsibility for the accuracy, completeness or usefulness of any information, apparatus, product or process disclosed, or represents that its use would not infringe privately owned rights.

Printed in the United States of America

Available from:

National Technical Information Service  
U.S. Department of Commerce  
5285 Port Royal Road  
Springfield, Virginia 22161

Price Printed Copy \$      \* ; Microfiche \$4.50

<u>*Pages</u>	<u>NTIS Selling Price</u>	
1-25	\$7.00	For documents over 500 pages, add \$1.50 for each additional 25-page increment.
25-50	\$8.50	
51-75	\$10.00	
76-100	\$11.50	
101-125	\$13.00	
126-150	\$14.50	
151-175	\$16.00	
176-200	\$17.50	
201-225	\$19.00	
226-250	\$20.50	
251-275	\$22.00	
276-300	\$23.50	
301-325	\$25.00	
326-350	\$26.50	
351-375	\$28.00	
376-400	\$29.50	
401-425	\$31.00	
426-450	\$32.50	
451-475	\$34.00	
476-500	\$35.50	
500-525	\$37.00	
526-550	\$38.50	
551-575	\$40.00	
567-600	\$41.50	

## Sawtooth Oscillation in Tokamaks

W. Park and D. A. Monticello  
Princeton Plasma Physics Laboratory  
Princeton, NJ 08543

### Abstract

A three-dimensional nonlinear toroidal full MHD code, *MHD3D*, has been used to study sawtooth oscillations in tokamaks. The profile evolution during the sawtooth crash phase compares well with experiment, but only if neoclassical resistivity is used in the rise phase. (Classical resistivity has been used in most of the previous theoretical sawtooth studies.) With neoclassical resistivity, the  $q$  value at the axis drops from 1 to about 0.8 before the crash phase, and then resets to 1 through a Kadomtsev-type complete reconnection process. This  $\Delta q_0 \simeq 0.2$  is much larger than  $\Delta q_0 \simeq 0.01$ , which is obtained if classical resistivity is used. The current profile is strongly peaked at the axis with a flat region around the singular surface, and is similar to the Textor profile. To understand this behavior, approximate formulas for the time behavior of current and  $q$  values are derived. A functional dependence of sawtooth period scaling is also derived. A semi-empirical scaling is found which fits the experimental data from various tokamaks. Some evidence is presented which indicates that the fast crash time is due to enhanced effective resistivity inside the singular current sheet, generated by, e.g., microinstability and electron parallel viscosity with stochastic fields at the x-point.

Since sawtooth oscillations<sup>1</sup> were first observed in tokamak experiments, Kadomtsev's model<sup>2</sup> had been successfully used to explain major features of the phenomenon. More recently, however, various new experimental features of sawteeth have been reported,<sup>3-5</sup> some seemingly contradicting the Kadomtsev model. Among these are the "anomalously" fast crash time,  $q$  value at the axis substantially below one, compound structures, and successor oscillations. To explain these features, alternative mechanisms have been proposed, some using modified Kadomtsev models,<sup>6,7</sup> and some using entirely different ones.<sup>5,8</sup>

In the present paper we show that the Kadomtsev model can explain most of the new experimental results. One basic difference in our study, which is crucial for the final conclusion, is the use of neoclassical resistivity. (Classical resistivity has been used in most previous theoretical sawtooth studies.) The main tool for the present study is a three-dimensional magnetohydrodynamic (MHD) code, *MH3D*.

The *MH3D* code solves the full nonlinear compressible resistive MHD equations in a three-dimensional toroidal geometry. The time step is limited by the shear Alfvén wave instead of the compressional wave. The stabilization of the compressional wave is achieved simply by making implicit the diagonal part of matrices which result from the compressional wave in the difference equations. This "quasi-implicit" scheme which was also used in our previous codes, *MH2D*<sup>9</sup> and *HIB*,<sup>10</sup> is found to be at least as effective for our code as the more elaborate "semi-implicit" scheme.<sup>11</sup> The large parallel thermal conductivity is accurately treated using the technique of artificial parallel sound as explained in Ref. 10.

The computer simulation closely mimics experiment, as the toroidal voltage at the wall (a boundary condition in the simulation) and the initial conditions determine the subsequent evolution of the plasma self-consistently. When an auxiliary heated plasma is simulated, a power deposition profile is required as input.

Figure 1 shows the X-ray traces during sawtooth oscillations in the simulation with Lundquist number  $S = 10^6$  and TFTR machine parameters. Figure 2 shows magnetic field puncture plots during a sawtooth crash, which correspond to a Kadomtsev-type complete reconnection. The ratio between the mixing radius to the  $q=1$  radius is about 1.4 in both the simulation and the corresponding experiment. (When classical resistivity is used in the sim-

ulation, this ratio is less than 1.2, as the resultant  $q$  profile inside the singular surface just before the crash is very flat and near one.) Temperature profile evolution during the crash phase compares well with experiment, both showing a hollow profile inside the island and in the final state.<sup>12</sup>

Figure 3 gives the  $q_0$  values at magnetic axes as a function of time. When two values of  $q_0$  are present at a given time, one is  $q_0$  of the magnetic island while the other is of the original main plasma. The drop of  $q_0$  of about 0.2 is found to be independent of the  $S$  value used in the calculation, because the sawtooth period scales as  $S$ , as explained later.

The drop in  $q$  of  $\Delta q_0 \simeq 0.2$  is more than an order of magnitude larger than  $\Delta q_0 \simeq 0.01$  which is obtained if classical resistivity is used, even though the neoclassical resistivity value itself is not much different from a classical one. This is because the neoclassical resistivity profile has a large second derivative near the axis that makes the current peak very quickly there, as shown in Fig. 4(a). (This head and shoulder type current profile has some similarity to Textor profiles.<sup>5</sup>) This gives the  $q$  profile of Fig. 4(b). This behavior can be understood quantitatively from the following derivation of its approximate time response.

Here it is sufficient to use a cylindrical model where the  $q = 1$  surface lies at  $r = r_s$ . By operating with  $\nabla^2$  on the flux equation with  $v_r = 0$ ,

$$\partial\psi/\partial t = \eta\nabla^2\psi = \eta J,$$

we obtain a toroidal current diffusion equation,

$$\partial J/\partial t = \nabla^2(\eta J).$$

For moderate inverse aspect ratio  $\epsilon$ ,  $\eta \simeq \eta_{\text{classical}}(T)/(1 - 2\sqrt{\epsilon})$ . This formula is matched smoothly to a thin transition layer at the axis ( $\epsilon \equiv r/R = 0$ ), where  $\eta \sim P(\epsilon^2)$  to ensure analytic behavior. Near the axis in ohmic plasmas, the variation of  $\eta$  due to temperature (T) dependence is much smaller than the variation due to  $\epsilon$  dependence from trapped particle effects. Hence, we assume that  $\eta$  is invariant in time. Multiplying both sides of the toroidal current diffusion equation by  $\eta$ , and introducing  $\xi \equiv \eta J$ , we obtain

$$\partial\xi/\partial t = \eta\nabla^2\xi.$$

The  $\xi$  profile inside the mixing radius just after the sawtooth crash is almost identical with that of  $\eta$  because  $J$  is almost constant there. [In the toroidal

case,  $RJ \simeq \text{Const.}$  as the dashed line in Fig. 4(a).] Given this initial condition, with a large second derivative near the axis, the above equation for  $\xi$  will give, to the leading order, flattening of  $\xi$  around the axis in a region  $r < r_t$  where  $r_t^2/\eta = t$  at time  $t$ . Thus  $J \propto \eta^{-1} \propto (1 - 2\sqrt{\epsilon})$  inside  $r = r_t$  will connect continuously to the  $r > r_t$  region where  $J \simeq 2$ . The transition layer of  $\eta$  at the axis will make the  $J$  profile smooth near the axis as shown in Fig. 4(a). Note that the peak value  $J_o$  stays the same because  $\eta(\epsilon = 0) = \eta_{\text{classical}}$ , independent of the transition layer thickness. (These characters also can be derived from the above procedure using a more accurate expression of  $\eta$  which explicitly describes the transition layer, as long as the layer thickness is smaller than  $r_t$ .) The value of  $J_o$  is then  $J_o \simeq 2/(1 - 2\sqrt{\epsilon_t})$ , where  $\epsilon_t \equiv r_t/R$ . The safety factor on axis,  $q_o(t)$ , is then

$$q_o(t) = 2/J_o(t) \simeq 1 - 2\sqrt{\epsilon_t} = 1 - 2\sqrt{\epsilon_s(t/\tau_R)}^{1/4},$$

where  $\epsilon_s \equiv r_s/R$  and the skin time is  $\tau_R \equiv r_s^2/\eta$ . This formula basically describes the behavior of  $q_o(t)$  shown in Fig. 3.

In light of the above, previous theoretical sawtooth studies<sup>6-8</sup> which rely on classical resistivity for their conclusions need to be reexamined. For example, Wesson,<sup>8</sup> using classical resistivity, assumed a very small  $\Delta q_o$  during the sawtooth period to arrive at his model of a fast sawtooth crash. Neoclassical resistivity, which should be valid for present-day large tokamaks, gives a  $\Delta q_o$  more than an order of magnitude larger.

The behavior of  $q_o(t)$  shown in Fig. 3 may also explain experimental results<sup>5</sup> which obtain  $q_o$  values much below one during the entire sawtooth period. Figure 3 shows that  $q_o$  stays much below one during a large portion of the sawtooth period. Due to the rapid initial drop of  $q_o$ , any measurement with substantial integration time will yield a value of  $q_o$  much below one.

The crash time of sawteeth has been called anomalously fast, and alternate models have been proposed to explain this time scale.<sup>7,8</sup> In our simulation, the crash phase corresponds to a complete reconnection process. In a reconnection process, the topology change may proceed with a time scale  $\tau_A$  (Petchek scaling),  $\tau_A^{1/2}\tau_R^{1/2}$  (Sweet-Parker scaling), or  $\tau_R$  (slow resistive time). It has been shown accurately in a two-dimensional cylindrical simulation that the  $m=1$  reconnection proceeds in the Sweet-Parker time scale ( $\tau_A^{1/2}\tau_R^{1/2}$ , or equivalently,  $\sim \eta^{1/2}$ ).<sup>13</sup> In our present three-dimensional simulation, the same time scaling is obtained. This time scale in typical TFTR parameters

is a few msec, if it is assumed that the resistivity inside the singular current sheet at the x-point is the same as in the bulk plasma. (Note that  $\eta$  in the above scalings represents the resistivity at the x-point.) However, inside the current sheet, the current density is orders of magnitude larger than in the bulk plasma and strong gradients of temperature and density exist. Thus a larger effective resistivity due to microinstability is likely. Moreover, since some stochasticity near the x-point is always present in a three-dimensional process, an increased effective resistivity due to electron parallel viscosity will be present at the x-point. A quantitative answer to this layer physics (which is lacking at the present) is necessary to estimate the reconnection time, and thus the sawtooth crash time. In TFTR discharges the sawtooth crash time varies anywhere between a few msec to tens of  $\mu\text{sec}$ . (The slower time matches the Sweet-Parker time with non-enhanced resistivity.) One prominent experimental feature is that a very fast crash sometimes immediately follows a slow crash and the resultant signals are indistinguishable from the slow case except for the crash time scale. It has been also shown that the temperature profiles during a very fast crash agree well with our three-dimensional simulation result using neoclassical resistivity. All these facts strongly suggest that the reconnection process with an enhanced effective resistivity at the x-point is responsible for the faster crash times observed in experiment.

One of the most important parameters of sawteeth which affect tokamak operation is the sawtooth period. For example, the ignition threshold for tokamak can depend on the length of the sawtooth period. Unfortunately, however, the sawtooth period has probably been the least understood part of the sawtooth mechanism. Our three-dimensional simulation results show that a sawtooth cycle consists of two distinctive stages. The first phase starts from the nearly toroidal symmetric state with the  $q$  value slightly higher than one inside the mixing radius (with  $q_0 = 1$ ), which results from the previous sawtooth crash. The second phase begins when the island starts to grow faster than the resistive time scale  $\tau_R$ . During the first stage, an island sometimes exists but its size changes only slowly in a time scale  $\geq \tau_R$ . There is no singular structure involved at this stage, thus the plasma evolution occurs in a  $\tau_R$  time scale. (The nonexistence of a singular structure has been tested by reducing  $\eta$  in the simulation.) During the second stage, the island grows and completely replaces in the original central region, in the Sweet-Parker

time scale,  $(\tau_A^{1/2} \tau_R^{1/2})$ . Since the first stage is much longer than the second crash stage, we can use the scaling of the duration of the first stage as the sawtooth period scaling.

As mentioned before, the first stage does not contain any singular structure, and thus evolves in the resistive time. This implies that the sawtooth period is proportional to the resistive time scale,  $\tau_{ST} \propto \tau_R \propto \eta^{-1}$ . This is the case in the simulation. (This differs from previous studies where the instability growth time determines the sawtooth period, which is then proportional to a fractional power of  $\eta^{-1}$ .<sup>14,15</sup>) Nonlinear stabilization, including the effect of the rapidly changing  $q$  profile, and low shear around the singular surface are probably responsible for the absence of a fast growing mode during the first stage.

We can deduce some additional functional dependence of the sawtooth period from the fact that the character of the neoclassical resistivity largely determines the evolution of the current profile, as mentioned in the derivation of  $q_o(t)$ . If we look at only the inside of the mixing radius during the first stage, the current profile at a given time,  $t$ , after the start of the first stage is approximately a function of  $(t/\tau_R)$  and the neoclassical resistivity profile with constant temperature. Here, the resistive time  $\tau_R$  is defined as  $\tau_R^2/\eta_o \propto \tau_s^2 Z_{o,eff}/T_o^{3/2}$ , where the subscript  $o$  means at the axis. Since the neoclassical resistivity profile is a function of  $\epsilon_s$ , the inverse aspect ratio of the singular surface,  $\epsilon_s$ , the inverse aspect ratio of the boundary layer at the axis, and the  $Z_{eff}$  profile, the time dependence of the  $q$  profile will be  $q(\epsilon, t) = F[(t/\tau_R), \epsilon_s, \epsilon_s, Z_{eff}(\epsilon)]$ . Then the functional dependence of the sawtooth period is

$$\tau_{ST} = \tau_R f[\epsilon_s, \epsilon_s, Z_{eff}(\epsilon)].$$

Here we have assumed that pressure effects are negligible. (This assumption seems to be valid even in a neutral-beam-heated TFTR plasma with peak  $\epsilon\beta_p = 0.1$ , in which case the simulation results indicate that the gross sawtooth mechanism is the same as in the zero  $\beta$  case.) We tried to find a specific scaling which fits preselected sawtooth period data of various tokamaks. It is found that a simple function,  $f = k\epsilon_s^{-2}$ , with the constant  $k$  obtained from the simulation shown in Fig 3, fits well with the experimental data as shown in Fig. 5. (The open circles are neutral-beam-heated cases.) This is a surprising result, because the data sets represent a wide range of  $\epsilon_s$  and presumably various  $Z_{eff}$  profiles. This semi-empirical scaling has numerical



values of

$$\tau_{ST} (\propto \epsilon_e^{-2} \tau_R) \approx 9R^2(T)^{3/2}/Z_{eff},$$

where  $\tau_{ST}$  is in msec, the major radius  $R$  in meters, and the peak electron temperature  $T$  in keV.

The data points of TFTR sawteeth need further explanation. These points represent the total duration of a compound sawtooth. The data points of non-compound sawteeth would lie below the scaling line and show a larger spread. This suggests that an intermediate relaxation mechanism tend to develop during a regular sawtooth oscillation as the Lundquist number  $S$  of the plasma becomes very large. This subordinate relaxation in the experiment disturbs only the annular region around the singular surface. It is possible that such a mode may indeed develop in the low shear annular region shown in Fig. 4 in a very high  $S$  regime. (Such a simulation takes a long computing time and will be studied in the future.) The previous picture of compound sawteeth relies on a hollow current profile which peaks off axis.<sup>16</sup> This is quite different from the simulated current profile shown in Fig. 4. One way a hollow current profile can occur is with a highly peaked impurity profile. However this is also unlikely since the previous sawtooth crash should eject any impurity accumulation.

Finally, some comments on the successor oscillation. We sometimes see a successor oscillation in the simulation, but only when the pressure is quite high. The mechanism responsible for the successor oscillation in our simulation is the saturation of the magnetic island due to pressure build up inside the island, as described in Ref. 9. In the present three-dimensional simulation this effect is essentially the same as the two-dimensional case studied in Ref. 9. This is because the basic mechanism of this saturation is a local effect, i.e., the change of the separatrix angle at the x-point from tangential to finite due to the pressure inside the island. The present MHD simulations using realistic experimental parameters (except the  $S$  value) did not produce any island saturation at zero  $\beta$ . This suggests that successor oscillations in ohmic plasmas may be due to non-MHD effects.

We wish to thank K. McGuire for experimental data, and A. Boozer, C.S. Chang, L. Chen, S. Jardin, H. Strauss, and R.B. White for helpful discussions. This work was supported by the United States Department of Energy under Contract DE-AC02-76-CHO-3073.

## References

- <sup>1</sup>S. von Goeler, W. Stodiek, and N.R. Sauthoff, *Phys. Rev. Lett.* **33**, 1201 (1974).
- <sup>2</sup>B.B. Kadomtsev, *Fiz. Plazmy* **1**, 710 (1975) [*Sov. J. Plasma Phys.* **1**, 389 (1975)].
- <sup>3</sup>K. McGuire et al., *12th European Conference on Controlled Fusion and Plasma Physics*, Budapest (1985).
- <sup>4</sup>A.W. Edwards et al., *Phys. Rev. Lett.* **57**, 210 (1986).
- <sup>5</sup>H. Soltwisch, W. Stodiek, J. Manickam, and J. Schluter, *Plasma Physics and Controlled Nuclear Fusion Research* (IAEA, Kyoto 1986), Vol. 1, p.263.
- <sup>6</sup>R.E. Denton, J.F. Drake, R.G. Kleva, and D.A. Boyd, *Phys. Rev. Lett.* **56**, 2477 (1986).
- <sup>7</sup>R.G. Kleva, J.F. Drake, and R.E. Denton, *Phys. Fluids* **30**, 2119 (1987).
- <sup>8</sup>J.A. Wesson, *Plasma Phys. Controlled Fusion* **28**, 243 (1986).
- <sup>9</sup>W. Park, D.A. Monticello, and T.K. Chu, *Phys. Fluids* **30**, 285 (1987).
- <sup>10</sup>W. Park, D.A. Monticello, H. Strauss, and J. Manickam, *Phys. Fluids* **29**, 1171 (1986).
- <sup>11</sup>D.S. Harned and D.D. Schnack, *J. Comput. Phys.* **65**, 57 (1986).
- <sup>12</sup>G. Kuo-Petravic et al., *Proceedings of Workshop on Resistive MHD*, Princeton, NJ, November (1988).
- <sup>13</sup>W. Park, D.A. Monticello, and R.B. White, *Phys. Fluids* **27**, 137 (1984).
- <sup>14</sup>G.L. Jahns, M. Soler, B.V. Waddell, J.D. Callen, and H.R. Hicks, *Nucl. Fusion* **18**, 609 (1978).
- <sup>15</sup>K. McGuire and D.C. Robinson, *Nucl. Fusion* **19**, 505 (1979).
- <sup>16</sup>V.V. Parail and G.V. Pereverzev, *Fiz. Plazmy* **6**, 27 (1980) [*Sov. J. Plasma Phys.* **6**, 14 (1980)].

## Figures

FIG. 1. Simulated soft X-ray traces.

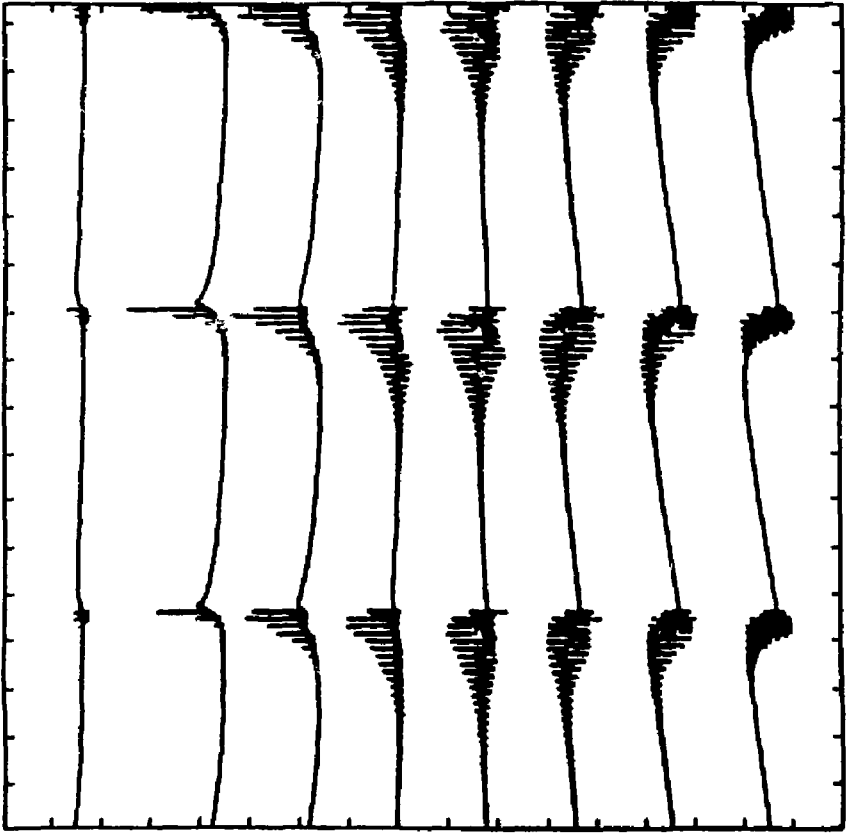
FIG. 2. Simulated magnetic field puncture plots during a crash phase.

FIG. 3. The  $q$  value at the axis versus time.

FIG. 4. Toroidal current and  $q$  profiles just before the crash.

FIG. 5. The semi-empirical sawtooth period scaling versus experimental val-  
ues.

#89T0058



TIME

Fig. 1

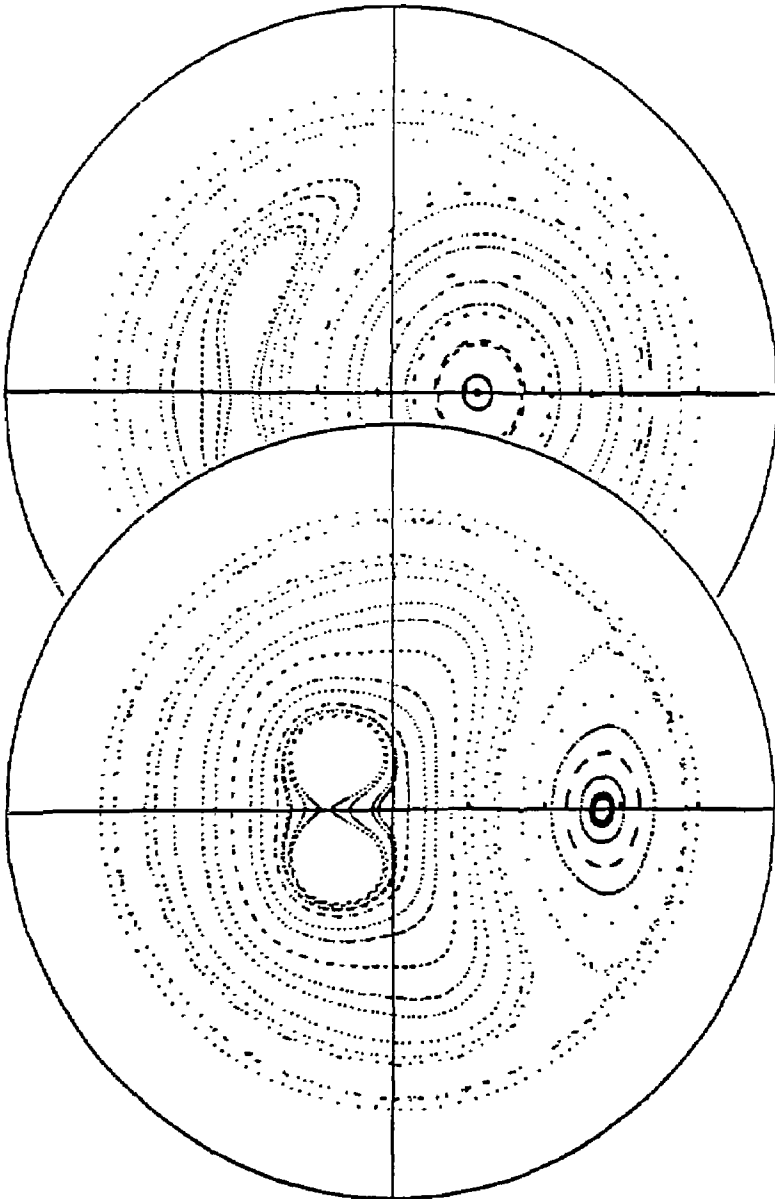


Fig. 2

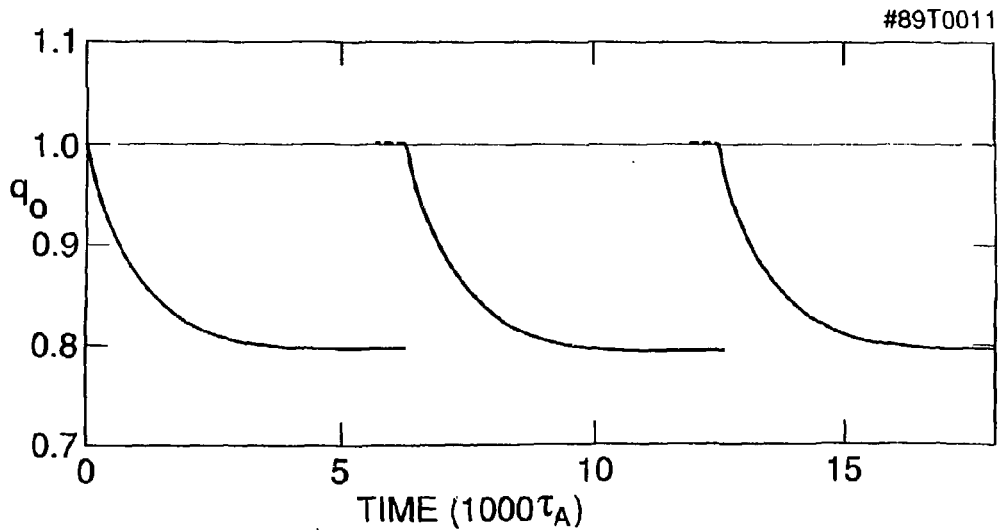


Fig. 3

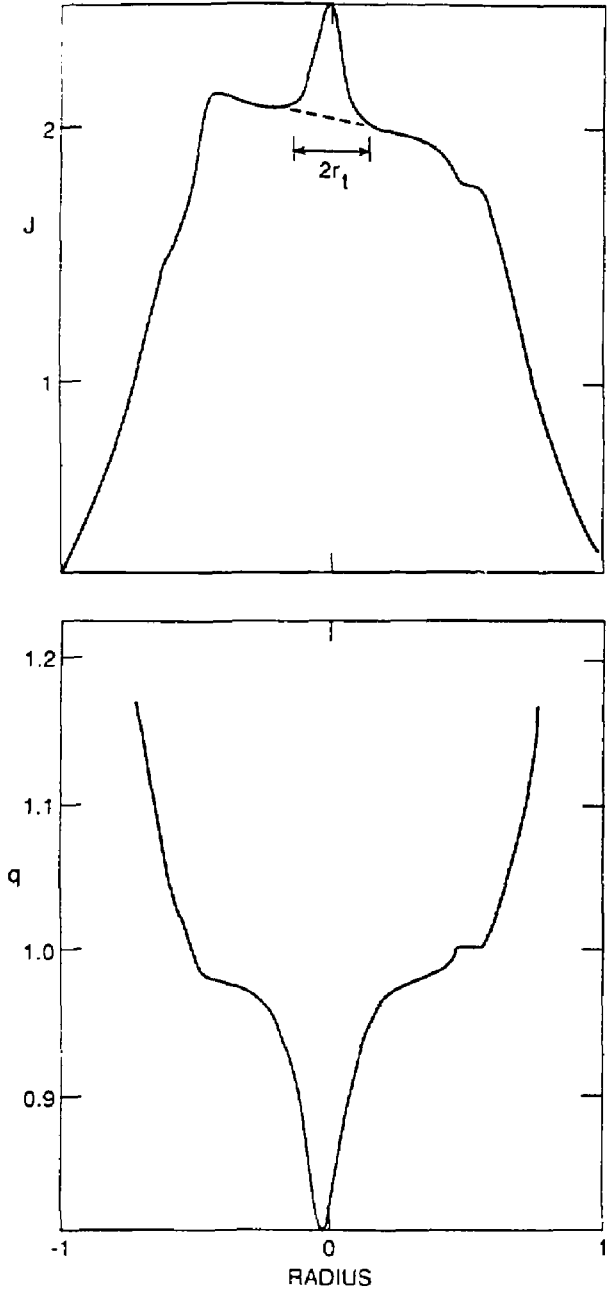


Fig. 4

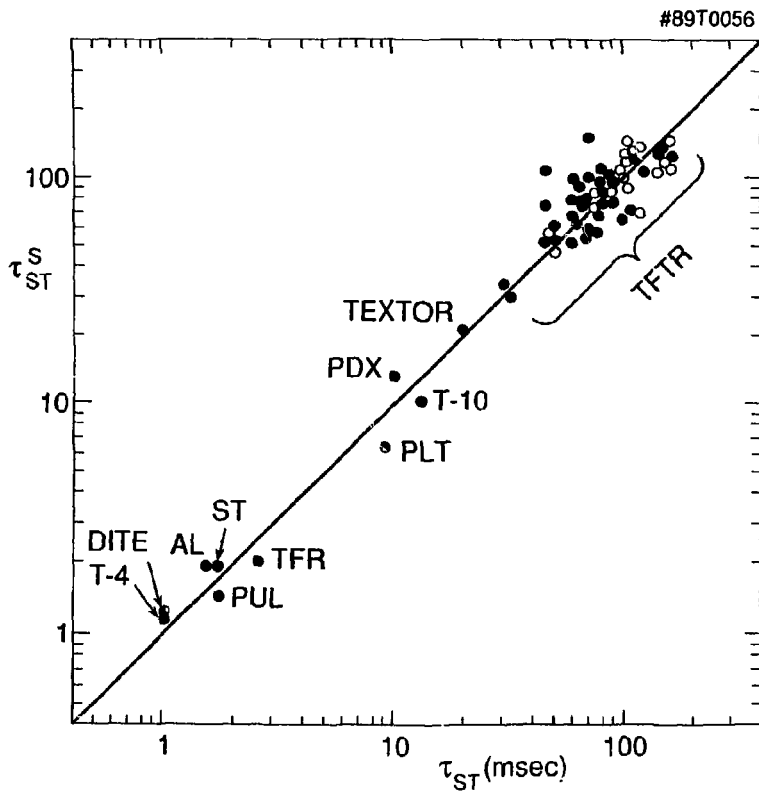


Fig. 5



EXTERNAL DISTRIBUTION IN ADDITION TO UC-420

Dr. Frank J. Paoloni, Univ of Wollongong, AUSTRALIA  
Prof. M.H. Brennan, Univ Sydney, AUSTRALIA  
Plasma Research Lab., Australian Nat. Univ., AUSTRALIA  
Prof. I.R. Jones, Flinders Univ., AUSTRALIA  
Prof. F. Cob, Inst Theo Phys, AUSTRIA  
Prof. M. Heindler, Institut für Theoretische Physik, AUSTRIA  
M. Goossens, Astronomisch Instituut, BELGIUM  
Ecole Royale Militaire, Lab de Phys Plasmas, BELGIUM  
Commission-Europeen, Dg-XII Fusion Prog, BELGIUM  
Prof. R. Boucique, Rijksuniversiteit Gent, BELGIUM  
Dr. P.H. Sakanaka, Instituto Fisica, BRAZIL  
Instituto De Pesquisas Espaciais-INPE, BRAZIL  
Documents Office, Atomic Energy of Canada Limited, CANADA  
Dr. N.P. Bchynski, MPB Technologies, Inc., CANADA  
Dr. H.M. Skarsgard, University of Saskatchewan, CANADA  
Dr. H. Barnard, University of British Columbia, CANADA  
Prof. J. Teichmann, Univ. of Montreal, CANADA  
Prof. S.R. Sreenivasan, University of Calgary, CANADA  
Prof. Tudor W. Johnston, INRS-Energie, CANADA  
Dr. Bolton, Centre canadien de fusion magnetique, CANADA  
Dr. C.R. James, Univ. of Alberta, CANADA  
Dr. Peter Lukac, Komenského Univ, CZECHOSLOVAKIA  
The Librarian, Culham Laboratory, ENGLAND  
The Librarian, Rutherford Appleton Laboratory, ENGLAND  
Mrs. S.A. Hutchinson, JET Library, ENGLAND  
C. Mouttet, Lab. de Physique des Milieux Ionisés, FRANCE  
J. Radet, CEN/CADARACHE - Bat 506, FRANCE  
Ms. C. Rinni, Librarian, Univ. of Ioannina, GREECE  
Dr. Tom Muel, Academy Bibliographic Ser., HONG KONG  
Preprint Library, Hungarian Academy of Sciences, HUNGARY  
Dr. B. Des Gupta, Saha Inst of Nucl. Phys., INDIA  
Dr. P. Kaw, Institute for Plasma Research, INDIA  
Dr. Philip Rosenau, Israel Inst. of Tech, ISRAEL  
Librarian, Int'l Ctr Theo Phys, ITALY  
Prof. G. Rostagni, Istituto Gas Ionizzati Del CNR, ITALY  
Miss Clelia De Palo, Assoc EURATOM-ENEA, ITALY  
Dr. G. Grosso, Istituto di Fisica del Plasma, ITALY  
Dr. H. Yamato, Toshiba Res & Dev, JAPAN  
Prof. I. Kawakami, Atomic Energy Res. Institute, JAPAN  
Prof. Kyoji Nishikawa, Univ of Hiroshima, JAPAN  
Director, Dept. Large Tokamak Res. JAERI, JAPAN  
Prof. Satoshi Itoh, Kyushu University, JAPAN  
Research Info Center, Nagoya University, JAPAN  
Prof. S. Tanaka, Kyoto University, JAPAN  
Library, Kyoto University, JAPAN  
Prof. Nobuyuki Inoue, University of Tokyo, JAPAN  
S. Mori, JAERI, JAPAN  
H. Jeong, Librarian, Korea Advanced Energy Res Inst, KOREA  
Prof. D.I. Choi, The Korea Adv. Inst of Sci & Tech, KOREA  
Prof. B.S. Lilley, University of Waikato, NEW ZEALAND  
Institute of Plasma Physics, PEOPLE'S REPUBLIC OF CHINA  
Librarian, Institute of Phys., PEOPLE'S REPUBLIC OF CHINA  
Library, Tsing Hua University, PEOPLE'S REPUBLIC OF CHINA  
Z. Li, Southwest Inst. Physics, PEOPLE'S REPUBLIC OF CHINA  
Prof. J.A.C. Cabral, Inst Superior Tecnico, PORTUGAL  
Dr. Octavian Petrus, AL I CUZA University, ROMANIA  
Dr. Jam de Villiers, Fusion Studies, AEC, SO AFRICA  
Prof. M.A. Hellberg, University of Natal, SO AFRICA  
C.I.E.M.A.T., Fusion Div. Library, SPAIN  
Dr. Lennart Stenflo, University of UMEA, SWEDEN  
Library, Royal Institute of Tech, SWEDEN  
Prof. Hans Wilhelmson, Chalmers Univ of Tech, SWEDEN  
Centre Phys des Plasmas, Ecole Polytech Fed, SWITZERLAND  
Bibliotheek, FOM-Inst Voor Plasma-Fysica, THE NETHERLANDS  
Metin Durgut, Middle East Technical University, TURKEY  
Dr. D.D. Ryutov, Siberian Acad Sci, USSR  
Dr. G.A. Eliseev, Kurchatov Institute, USSR  
Dr. V.A. Glukhikh, Inst Electrophysical Apparatus, USSR  
Prof. O.s. Padichenko, Inst. of Phys. & Tech. USSR  
Dr. L.M. Kovrizhnykh, Institute of Gen. Physics, USSR  
Nuclear Res. Establishment, Julich Ltd., W. GERMANY  
Bibliotheek, Inst. Fur Plasmaforschung, W. GERMANY  
Dr. K. Schindler, Ruhr-Universität Bochum, W. GERMANY  
ASDEX Reading Rm, c/o Wagner, IPP/Max-Planck, W. GERMANY  
Librarian, Max-Planck Institut, W. GERMANY  
Prof. R.K. Jansev, Inst of Phys, YUGOSLAVIA